

Supplementary Information

Identifying isomers of peroxy radicals in the gas phase: 1-C₃H₇O₂ vs 2-C₃H₇O₂

Xiaofeng Tang,^{*a} Xiaoxiao Lin,^a Gustavo A. Garcia,^b Jean-Christophe Loison,^c Zied Gouid,^{d,g} Hassan H. Abdallah,^e Christa Fittschen,^f Majdi Hochlaf,^{*d} Xuejun Gu,^a Weijun Zhang^a and Laurent Nahon^{*c}

Experimental and Theoretical Details

Experiments were carried out with the i²PEPICO spectrometer, DELICIOUS III, on the undulator-based VUV beamline DESIRS at synchrotron SOLEIL, France.^{1, 2} Synchrotron radiation photons were dispersed by a 6.65 m normal incidence monochromator with a 200 l.mm⁻¹ grating and the photon energy resolution was set at ~3 meV. A gas filter filled with Kr was utilized to suppress high harmonics emitted from the undulator that could be transmitted by the grating's high-orders. A flow tube was employed as chemical reactor to model and study the low temperature oxidation of propane, in which fluorine atoms produced from diluted F₂ gas in helium (5%, 15 sccm) with a microwave discharge generator (Sairem, 2.45 GHz) were used to initiate reactions.^{3,4} Reactants like propane and oxygen, together with helium carrier gas, were added and the total gas flow rate was fixed at 1600 sccm with a 2 mbar pressure inside the flow tube. The gas mixture was sampled through two skimmers (1 mm diameter) and crossed the photon beam at the center of DELICIOUS III,^{2,5} where photoelectrons and photoions produced by photoionization were extracted and accelerated in opposite directions towards an electron velocity map imaging (VMI) device and a modified Wiley-McLaren ion momentum imager analyzer. The ion 3D velocity distribution is derived from the TOF and the arrival position. The photoelectron images were filtered by ion mass and velocity, and subsequently Abel inverted⁶ to obtain the electron kinetic energy distribution and TPES.

Computations consisted of the determinations of the structures of the neutral and ionic species of $C_3H_7O_2$ sum formula and of the corresponding the adiabatic ionization energies (AIEs), potential energy curves and Franck-Condon factors. Concretely, the geometry optimizations, without constraints (in the C_1 point group), of the stable forms of the neutral and the cationic species of $C_3H_7O_2$, followed by (an)harmonic frequency computations to ensure the minimal nature of the optimized structures, were done at the PBE0/aug-cc-pVDZ level as implemented in the GAUSSIAN 09 program package.⁷ We also performed full optimization of the structures at the explicitly correlated coupled cluster single-double and perturbative triple excitations approach, (R)CCSD(T)-F12 in conjunction with the aug-cc-pVTZ basis set⁸ as implemented in MOLPRO 2015⁹. Afterwards, we derived the AIEs of the $C_3H_7O_2$ isomers using either the PBE0/aug-cc-pVDZ(opt)//(R)CCSD(T)-F12/aug-cc-pVDZ(SP)^{10, 11} composite scheme or at the (R)CCSD(T)-F12/aug-cc-pVDZ level (denoted (R)CCSD(T)-F12 /aug-cc-pVDZ (opt)). Within the composite scheme, single point (SP) calculations using the (R)CCSD(T)-F12/aug-cc-pVTZ approach⁸, are done at the PBE0/aug-cc-pVDZ optimized geometries. The full set of results are listed in Table S1 and Table S2. The composite scheme PBE0/aug-cc-pVDZ(opt)//(R)CCSD(T)-F12/aug-cc-pVDZ(SP)^{10, 11} is viewed to allow derivation of accurate energetics up to ± 0.02 eV (including AIEs) as established for a wide range of small and medium sized compounds, also including “unstable” radicals and ions.^{12, 13} Worth noting the good performance of the less computationally demanding PBE0/aug-cc-pVDZ (optg)//(R)CCSD(T)-F12/aug-cc-pVTZ (SP)+ZPVE (PBE0/aug-cc-pVDZ) composite scheme with respect to the costly (R)CCSD(T)-F12/aug-cc-pVTZ (optg)+ZPVE (PBE0/aug-cc-pVDZ) approach.

The Franck-Condon factors for the ionization transitions of $C_3H_7O_2$, as well as for the geometry and harmonic frequency calculations required as input parameters, were calculated at the M062X/aug-cc-pVTZ level of theory using the time-independent adiabatic Hessian Franck-Condon model in the GAUSSIAN program.⁷ The data are given in Fig. 3.

The potential energy curves of the low-lying electronic states of the neutral and the cationic $C_3H_7O_2$ along the C-O coordinate (Fig. S2) were calculated at the QCISD(T)/cc-pVTZ level of theory in the GAUSSIAN program.⁷

Results

Table S1. Computed equilibrium structures of the isomers and rotamers of the propylperoxy radical, together with their cations, obtained at the PBE0/aug-cc-pVDZ and (R)CCSD(T)-F12/aug-cc-pVDZ levels of theory. We give also their PBE0/aug-cc-pVDZ total energies (in Hartree) and zero point vibrational energies ZPVE (in eV) and (R)CCSD-F12(T)/aug-cc-pVDZ computations total energies (in Hartree). For the propylperoxy radical, we used the denomination of Tarczay *et al.*¹⁴ for the isomers and rotamers. For the neutrals we computed the lowest doublet state and for the cation we computed the lowest singlet state.

Method/basis set	1-C ₃ H ₇ O ₂ neutral species				
	G ₁ G ₂	G ₁ T ₂	T ₁ G ₂	G' ₁ G ₂	T ₁ T ₂
PBE0/aug-cc-pVDZ (opt) ^[a]	-268.58289042	-268.58282837	-268.58245543	-268.58207934	-268.5823823
ZPVE /PBE0/aug-cc-pVDZ (opt) ^[a]	2.73	2.73	2.72	2.72 2.76 ^[c]	2.72
RCCSD(T)-F12 /aug-cc-pVDZ (SP) ^[b]	-268.47907369	-268.47882282	-268.47848217	-268.47828718	-268.47827678
RCCSD(T)-F12 /aug-cc-pVDZ (opt) ^[a]	-268.47941948	-268.47915014	-268.47884503	-268.47862173	-268.47862221
Relative energy (cm ⁻¹) ^{[a], [d]}	0	59	126	175	175
	1-C ₃ H ₇ O ₂ ⁺ ionic species				
	G _{1a} T ₂ ⁺	G _{1b} T ₂ ⁺	G _{1c} T ₂ ⁺	G _{1a} G ₂ ⁺	G _{1b} G ₂ ⁺
PBE0/aug-cc-pVDZ (opt) ^[a]	-268.2124092	-268.212061812	-268.4534305 ^[c]	-268.21096674	-268.4571536 ^[c]
ZPVE /PBE0/aug-cc-pVDZ (opt) ^[a]	2.70	2.64	2.72 ^[c]	2.69	2.72 ^[c]
CCSD(T)-F12 /aug-cc-pVDZ (SP) ^[b]	-268.11341454	-268.11302719	-	-268.11201897	-

CCSD(T)-F12 /aug-cc-pVDZ (opt) ^[a]	-268.11496856	-268.11479234	-268.11438085	-268.11395345	-268.11702749
	2-C₃H₇O₂ neutral species		2-C₃H₇O₂⁺ ionic species		
	G	T	T⁺	G⁺	
PBE0/aug-cc-pVDZ (opt) ^[a]	-268.5886508	-268.58801268	-268.2242517	-268.2213351	
ZPVE /PBE0/aug-cc-pVDZ (opt) ^[a]	2.70	2.71	2.67	2.67	
(R)CCSD(T)-F12 /aug-cc-pVDZ (SP) ^[b]	-268.48532326	-268.48469911	-268.12587128	-268.12535720	
(R)CCSD(T)-F12 /aug-cc-pVDZ (opt) ^[a]	-268.48567130	-268.48502450	-268.12745737	-268.12652401	
Relative energy (cm ⁻¹) ^{[a], [d]}	0	142			

[a] Full optimisation.

[b] Single point computations at the PBE0/aug-cc-pVDZ optimized geometry.

[c] Optimised at the M06-2X/aug-cc-pTVZ level of theory.

[d] Relative energy to the most stable rotamer.

Table S2. Calculated adiabatic ionisation energies (AIEs, eV) of the propylperoxy radicals' isomers and rotamers. See Table S1 for details.

Photoionization transition ^[a]	AIE ^[b]	AIE ^[c]
1-C₃H₇O₂		
G₁G₂ → G_{1a}T₂⁺	9.92	9.88
G₁T₂ → G_{1a}T₂⁺	9.90	9.88
T₁G₂ → G_{1a}T₂⁺	9.91	9.88
G'₁G₂ → G_{1a}T₂⁺	9.92	9.87
T₁T₂ → G_{1a}T₂⁺	9.90	9.87
G₁G₂ → G_{1a}G₂⁺	9.94	9.90
G₁T₂ → G_{1a}G₂⁺	9.94	9.90
T₁G₂ → G_{1a}G₂⁺	9.94	9.90
G'₁G₂ → G_{1a}G₂⁺	9.93	9.89
T₁T₂ → G_{1a}G₂⁺	9.93	9.89
G₁T₂ → G_{1b}T₂⁺	9.86	9.82
2-C₃H₇O₂		
G → G⁺	9.76	9.74
G → T⁺	9.75	9.71
T → G⁺	9.73	9.71
T → T⁺	9.72	9.69

[a] To populate the lowest singlet cationic state a¹A'.

[b] Using the PBE0/aug-cc-pVDZ (optg)//(R)CCSD(T)-F12/aug-cc-pVTZ (SP)+ZPVE (PBE0/aug-cc-pVDZ) composite scheme.

[c] Using the (R)CCSD(T)-F12/aug-cc-pVTZ (optg)+ZPVE (PBE0/aug-cc-pVDZ or M06-2X/AVTZ) level composite scheme

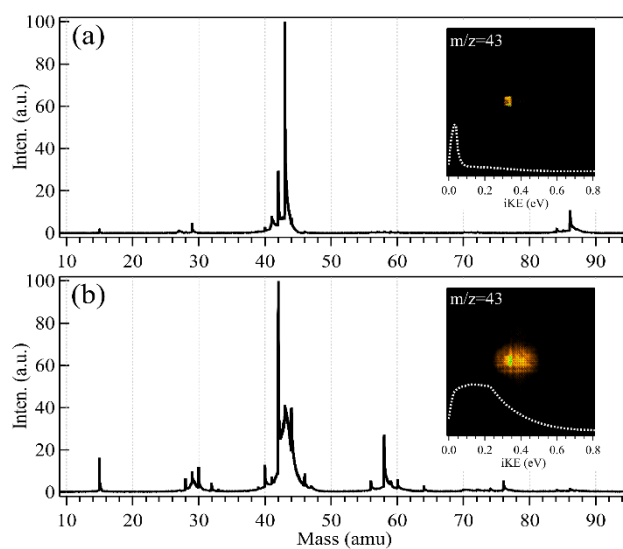


Fig. S1 Photoionization TOF mass spectra and the m/z 43 ion images acquired (a) without (integrated in the 7.2-11 eV range) and (b) with (integrated in the 9-11 eV range) addition of oxygen into the flow tube, together with its kinetic energy distributions (iKE, white dashed lines).

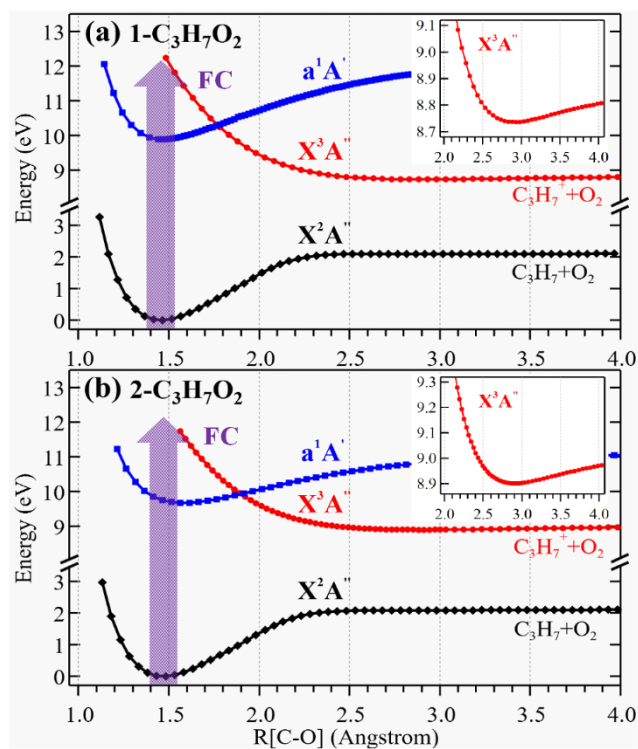


Fig. S2 Potential energy curves of (a) the G_1G_2 rotamer of $1\text{-C}_3\text{H}_7\text{O}_2$ and (b) the G rotamer of $2\text{-C}_3\text{H}_7\text{O}_2$, and their cations along the C-O coordinates, together with a zoom on the cationic ground state minima. The Franck-Condon (FC) region is displayed as a purple arrow.

References

- 1 L. Nahon, N. de Oliveira, G. A. Garcia, J. F. Gil, B. Pilette, *et al.*, *J. Synchrotron Rad.*, 2012, **19**, 508.
- 2 G. A. Garcia, B. K. C. de Miranda, M. Tia, S. Daly and L. Nahon, *Rev. Sci. Instrum.*, 2013, **84**, 053112.
- 3 G. A. Garcia, X. Tang, J.-F. Gil, L. Nahon, M. Ward, *et al.*, *J. Chem. Phys.*, 2015, **142**, 164201.
- 4 X. Tang, X. Gu, X. Lin, W. Zhang, G. A. Garcia, *et al.*, *J. Chem. Phys.*, 2020, **152**, 104301.
- 5 X. Tang, G. A. Garcia, J. F. Gil and L. Nahon, *Rev. Sci. Instrum.*, 2015, **86**, 123108.
- 6 G. A. Garcia, L. Nahon and I. Powis, *Rev. Sci. Instrum.*, 2004, **75**, 4989.
- 7 M. J. Frisch, G. W. Trucks, H. B. Schlegel, G. E. Scuseria, M. A. Robb, *et al.*, *Gaussian 09, Revision A02*. Gaussian, Inc., Wallingford CT, 2016.
- 8 Q. Ma and H.-J. Werner, *Wiley Interdis. Rev.: Comput. Mol. Sci.*, 2018, **8**, e1371.
- 9 H.-J. Werner and P. J. Knowles, *MOLPRO version 2015*, MOLPRO version 2015, <http://www.molpro.net>.
- 10 M. Hochlaf, *Phys. Chem. Chem. Phys.*, 2017, **19**, 21236.
- 11 M. Hochlaf, *Physics of Life Reviews*, 2020, **32**, 101.
- 12 H. Y. Zhao, K.-C. Lau, G. A. Garcia, L. Nahon, S. Carniato, *et al.*, *Phys. Chem. Chem. Phys.*, 2018, **20**, 20756.
- 13 I. Derbali, H. R. Hrodmarsson, Z. Gouid, M. Schwell, M.-C. Gazeau, *et al.*, *Phys. Chem. Chem. Phys.*, 2019, **21**, 14053.
- 14 G. Tarczay, S. J. Zalyubovsky and T. A. Miller, *Chem. Phys. Lett.*, 2005, **406**, 81.